

Thermal post-buckling analysis of functionally graded beams with temperature-dependent physical properties

Turgut KOCATÜRK* and Şeref Doğuşcan AKBAŞ

*Yıldız Technical University, Davutpaşa Campus, Department of Civil Engineering,
34210 Esenler-Istanbul, Turkey*

(Received October 12, 2012, Revised July 14, 2013, Accepted August 01, 2013)

Abstract. This paper focuses on thermal post-buckling analysis of functionally graded beams with temperature dependent physical properties by using the total Lagrangian Timoshenko beam element approximation. Material properties of the beam change in the thickness direction according to a power-law function. The beam is clamped at both ends. In the case of beams with immovable ends, temperature rise causes compressible forces and therefore buckling and post-buckling phenomena occurs. It is known that post-buckling problems are geometrically nonlinear problems. Also, the material properties (Young's modulus, coefficient of thermal expansion, yield stress) are temperature dependent: That is the coefficients of the governing equations are not constant in this study. This situation suggests the physical nonlinearity of the problem. Hence, the considered problem is both geometrically and physically nonlinear. The considered highly non-linear problem is solved considering full geometric non-linearity by using incremental displacement-based finite element method in conjunction with Newton-Raphson iteration method. In this study, the differences between temperature dependent and independent physical properties are investigated for functionally graded beams in detail in post-buckling case. With the effects of material gradient property and thermal load, the relationships between deflections, critical buckling temperature and maximum stresses of the beams are illustrated in detail in post-buckling case.

Keywords: functionally graded material; temperature dependent physical properties; thermal post-buckling analysis; total lagrangian finite element model

1. Introduction

Functionally graded materials (FGMs) are a new generation of composites where the volume fraction of the FGM constituents vary gradually, giving a non-uniform microstructure with continuously graded macro properties such as elasticity modulus, density, heat conductivity, etc. Typically, in an FGM, one face of a structural component is ceramic that can resist severe thermal loading and the other face is metal which has excellent structural strength. FGMs consisting of heat-resisting ceramic and fracture-resisting metal can improve the properties of thermal barrier systems because cracking and delamination, which are often observed in conventional layered

*Corresponding author, Professor, E-mail: kocaturk@yildiz.edu.tr

^a Ph.D., E-mail: serefdada@yahoo.com

composites, are reduced by proper smooth transition of material properties. FGMs have many practical applications, such as reactor vessels, biomedical sectors, aircrafts, space vehicles, defense industries and other engineering structures. As nuclear power plants, aerospace vehicles, thermal power plants etc. are subjected to large thermal loadings, FGMs have found extensive applications in these applications. The design of FGM structural elements (beams, plates, shells etc.) in the high thermal environments is very important. Especially, in the case of structural elements with immovable ends, temperature rise causes compressible forces end therefore buckling and post-buckling phenomena occurs. With the increased use of FGMs, understanding the mechanical behavior of FG structures is very important. It is known that buckling and post-buckling problems are nonlinear problems. In recent years, with the development of technology in aerospace engineering, structural engineering, robotics and manufacturing make it inevitable to excessively use non-linear models that must be solved numerically. Because, closed-form solutions of non-linear problems of beams with general loading and boundary conditions using elliptic integrals are limited.

In recent years, much more attention has been given to the thermal buckling of FG beam structures. Thermal buckling of thick, moderately thick and thin cross-ply laminated beams subjected to uniform temperature distribution is analyzed by Khdeir (2001). Thermoelastic equilibrium equations for a functionally graded beam are solved in closed-form to obtain the axial stress distribution by Sankar and Tzeng (2002). Thermal buckling load of a curved beam made of functionally graded material with doubly symmetric cross section is investigated by Rastgo *et al.* (2005). Li *et al.* (2006) analyzed thermal post-buckling of Functionally Graded clamped-clamped Timoshenko beams subjected to transversely non-uniform temperature. Buckling and vibration behaviour of a functionally graded sandwich beam having constrained viscoelastic layer is studied in thermal environment by using finite element formulation by Bhangale and Ganesan (2006). Nirmula *et al.* (2006) derived analytical expressions for the thermo-elastic stresses in a three-layered composite beam system whose middle layer is a functionally graded material. Three-dimensional thermal buckling and postbuckling analyses of functionally graded materials subjected to uniform or non-uniform temperature rise are examined by using finite element method by Na and Kim (2006). Two-dimensional thermoelasticity analysis of functionally graded thick beams is presented using the state space method coupled with the technique of differential quadrature by Lu *et al.* (2006). Thermoelastic stress field in a functionally graded curved beam, where the elastic stiffness varies in the radial direction, is considered by Mohammadia and Drydena (2008). Rahimi and Davoodinik (2008) studied thermal behaviour analysis of the functionally graded Timoshenko beam. A third-order zigzag theory based finite element model in conjunction with the modified rule of mixtures and Wakashima–Tsukamoto model for estimating effective modulus of elasticity and coefficient of thermal expansion, respectively, is presented for layered functionally graded beams under thermal loading by Kapuria *et al.* (2008). Based on Kirchhoff's assumption of straight normal line of beams and considering the effects of the axial elongation, the initial curvature and the stretching-bending coupling on the arch deformation, geometrically nonlinear governing equations of functionally graded arch subjected to mechanical and thermal loads are derived by Song and Li (2008). Lim *et al.* (2009) investigated temperature-dependent in-plane vibration of functionally graded (FGM) circular arches based on the two-dimensional theory of elasticity. Buckling of beams made of functionally graded material under various types of thermal loading is studied based on the Euler–Bernoulli beam theory by Kiani and Eslami (2010). Thermal post-buckling behaviour of uniform slender FG beams is investigated independently using the classical Rayleigh-Ritz (RR) formulation and the versatile

finite element analysis based on the von-Karman strain-displacement relations by Anand Rao *et al.* (2010). Free vibration analysis of initially stressed thick simply supported functionally graded curved panel resting on two-parameter elastic foundation (Pasternak model), subjected in thermal environment is studied using the three-dimensional elasticity formulation by Farid *et al.* (2010). Akbaş and Kocatürk (2011) investigated post-buckling analysis of a simply supported beam subjected to a uniform thermal loading by using total Lagrangian finite element model of two dimensional continuum for an eight-node quadratic element. Kocatürk and Akbaş (2011) studied post-buckling analysis of Timoshenko beams with various boundary conditions subjected to a non-uniform thermal loading by using the total Lagrangian Timoshenko beam element approximation. Akbaş and Kocatürk (2012) discussed thermal post buckling of 2-D functionally graded beams. Akbaş (2012) studied thermal post-buckling of functionally graded beams. Kocatürk and Akbaş (2012) investigated post-buckling analysis of functionally graded Timoshenko beams under thermal loadings. In a recent study, Akbaş and Kocatürk (2012) examined post-buckling behavior of Timoshenko beams subjected to uniform temperature rising with temperature dependent physical properties.

It is seen from literature that post-buckling studies with temperature-dependent physical properties for functionally graded beams has not been broadly investigated. Post-buckling behavior of functionally graded Timoshenko beams subjected to temperature rising with temperature dependent physical properties are studied in this paper by using the total Lagrangian Timoshenko beam element approximation. The considered highly non-linear problem is solved considering full geometric non-linearity by using incremental displacement-based finite element method in conjunction with Newton-Raphson iteration technique. The distinctive feature of this study is post-buckling analysis of functionally graded Timoshenko beams under thermal loading considering full geometric non-linearity and temperature dependent physical properties by using the total Lagrangian finite element model of Timoshenko beam. The differences of the analysis results in the case of temperature dependent and independent physical properties are investigated in detail in post-buckling case for functionally graded beams.

The development of the formulations of general solution procedure of nonlinear problems follows the general outline of the derivation given by Zienkiewicz and Taylor (2000). The related formulations of post-buckling analysis of Timoshenko beams with various boundary conditions subjected to a non-uniform thermal loading are obtained by using the total Lagrangian finite element model of Timoshenko beam. In deriving the formulations for post buckling analysis under uniform thermal loading and temperature dependent physical properties for FGM, the total Lagrangian Timoshenko beam element formulations given by Felippa (2012) are used. There is no restriction on the magnitudes of deflections and rotations in contradistinction to von-Karman strain displacement relations of the beam. The difference between temperature dependent and independent physical properties are investigated in detail in post-buckling case. The relationships between deflections, critical buckling temperature, maximum stresses of the beams and temperature rising are illustrated in detail in post-buckling case.

2. Theory and Formulations

The clamped-clamped beam configurations, with co-ordinate system O (X,Y,Z) are shown in Fig. 1.

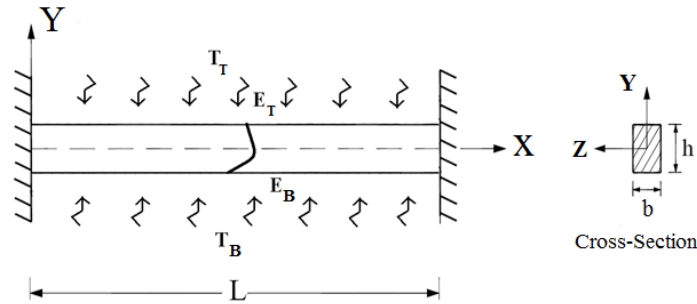


Fig. 1 Clamped-clamped FG beam subjected to temperature rising and cross-section

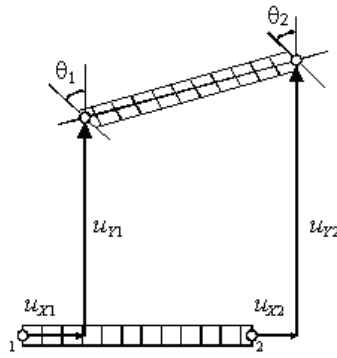


Fig. 2 A two-node C^0 beam element

In this study, the Total Lagrangian Timoshenko beam element is used and the related formulations are developed for temperature dependent physical properties by using the formulations given by Kocatürk and Akbaş (2012) which was developed for thermal loading by using the formulations given by Felippa (2012). In the present study, finite element model of Timoshenko beam element is developed by using a two-node beam element shown in Fig. 2. Each node has three degrees of freedom: Two node displacements u_{xi} and u_{yi} , and one rotation q_i about Z axis.

In this study, the material properties are both temperature-dependent and position-dependent. The effective material properties of the FG beam, P , i.e., Young's modulus E , coefficient of thermal expansion α_x , coefficient of thermal conductivity k , temperature rise T , yield stress σ_y and shear modulus G vary continuously in the thickness direction (Y axis) according to a power-law function and a function of temperature T as follows

$$P(Y, T) = (P_T(T) - P_B(T)) \left(\frac{Y}{h} + \frac{1}{2} \right)^n + P_B(T) \tag{1}$$

where P_T and P_B are the material properties of the top and the bottom surfaces of the beam that depends on temperature (T). It is clear from Eq. (1) that when $Y = -h/2$, $P = P_B$, and when $Y = h/2$, $P = P_T$. Where n is the non-negative power-law exponent which dictates the material variation profile through the thickness of the beam.

The beams considered in numerical examples are made of Austenitic Stainless Steel (316) and pure Molybdenum. The bottom surface of the functionally graded beam is pure Molybdenum and the top surface of the functionally graded beam is Austenitic Stainless Steel-316.

The coefficients of temperature T for Austenitic Stainless Steel (316) are expressed as follows (from Incropera and DeWitt (1985), Detail of the ITER Outline Design Report (1994), ITER Documentation Series: No. 29 (1991), ASME Code Cases: Nuclear Components (1992))

$$E(T) = 205.91 - 2.6913 \times 10^{-2} T - 4.1876 \times 10^{-5} T^2 \quad (\text{Gpa}) \quad (2a)$$

$$\alpha(T) = (11.813 + 1.3106 \times 10^{-2} T - 6.1375 \times 10^{-6} T^2) \times 10^{-6} \quad (1/\text{K}) \quad (2b)$$

$$k(T) = 9.0109 + 1.5298 \times 10^{-2} T \quad (\text{W/mK}) \quad (2c)$$

$$\sigma_y(T) = 448.69 - 1.193T + 1.4787 \times 10^{-3} T^2 - 6.3134 \times 10^{-7} T^3 \quad (\text{Mpa}) \quad (2d)$$

where E is Young's modulus, α_x is thermal expansion coefficient, k coefficient of thermal conductivity and σ_y is yield stress. Poisson's ratio is taken as $\nu = 0.27$. In this study, the unit of the temperature is taken as Kelvin (K). These equations are valid for temperatures ranging from 300 K to 1000 K.

The coefficients of temperature T for pure Molybdenum are expressed as follows (from Shinno *et al.* (1988), Detail of the ITER Outline Design Report (1994), ITER Documentation Series: No. 29 (1991), Hashizume and Miya (1987), Tietz and Wilson (1965))

$$E(T) = 338.93 - 3.413 \times 10^{-2} T - 8.2007 \times 10^{-6} T^2 \quad (\text{Gpa}) \quad (3a)$$

$$\alpha(T) = (4.9904 + 1.1837 \times 10^{-4} T - 3.5877 \times 10^{-7} T^2) \times 10^{-6} \quad (1/\text{K}) \quad (3b)$$

$$k(T) = 152.78 - 5.0884 \times 10^{-2} T + 9.6754 \times 10^{-6} T^2 \quad (\text{W/mK}) \quad (3c)$$

$$\sigma_y(T) = 309.75 + 0.165T - 3.675 \times 10^{-4} T^2 + 1.0535 \times 10^{-7} T^3 \quad (\text{Mpa}) \quad (3d)$$

These equations are valid for temperatures ranging from 300 K to 2100 K.

A particle originally located at $P_0(X, Y)$ moves to $P(x, y)$ in the current configuration, as shown in Fig. 3. The projections of P_0 and P along the cross sections at C_0 and C upon the neutral axis are called $C_0(X, 0)$ and $C(x_c, y_c)$, respectively. It will be assumed that dimensions of the beam cross section do not change, and that the shear distortion $\gamma \ll 1$ so that $\cos \gamma$ can be replaced by 1. Felippa (2012).

$$x = x_c - Y(\sin \psi + \sin \gamma \cos \psi) = x_c - Y[\sin(\psi + \gamma) + (1 + \cos \gamma) \sin \psi] = x_c - Y \sin \theta \quad (4)$$

$$y = y_c - Y(\cos \psi + \sin \gamma \sin \psi) = x_c - Y[\cos(\psi + \gamma) + (1 + \cos \gamma) \cos \psi] = y_c - Y \cos \theta \quad (5)$$

where $x_c = X + u_{XC}$ and $y_c = u_{YC}$. Consequently, $x = X + u_{XC} - Y \sin \theta$ and $y = u_{YC} + Y \cos \theta$. From now on we shall call u_{XC} and u_{YC} simply u_X and u_Y , respectively, so that the Lagrangian representation of the motion is

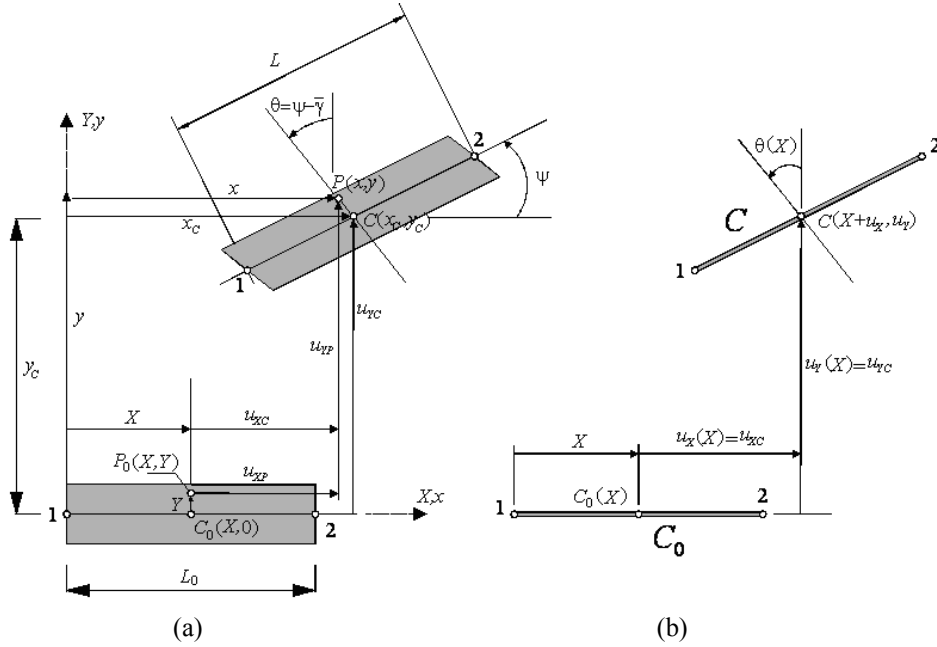


Fig. 3 Lagrangian kinematics of the C^0 beam element with X -aligned reference configuration: (a) plane beam moving as a two-dimensional body; (b) reduction of motion description to one dimension measured by coordinate X . This figure is given by Felippa (2012)

$$\begin{bmatrix} x \\ y \end{bmatrix} = \begin{bmatrix} X + u_x - Y \sin \theta \\ u_y + Y \cos \theta \end{bmatrix} \quad (6)$$

in which u_x , u_y and θ are functions of X only. This concludes the reduction to a one-dimensional model, as sketched in Fig. 3(b). For a two-node C_0 element, it is natural to express the displacements and rotation functions as linear in between the node displacements

$$w = \begin{bmatrix} u_x(X) \\ u_y(X) \\ \theta(X) \end{bmatrix} = \frac{1}{2} \begin{bmatrix} 1-\zeta & 0 & 0 & 1+\zeta & 0 & 0 \\ 0 & 1-\zeta & 0 & 0 & 1+\zeta & 0 \\ 0 & 0 & 1-\zeta & 0 & 0 & 1+\zeta \end{bmatrix} \begin{bmatrix} u_{X1} \\ u_{Y1} \\ \theta_1 \\ u_{X2} \\ u_{Y2} \\ \theta_2 \end{bmatrix} = Nu \quad (7)$$

in which $\zeta = (2X/L_0) - 1$ is the isoparametric coordinate that varies from $\zeta = -1$ at node 1 to $\zeta = 1$ at node 2.

The Green-Lagrange strains are given as follows Felippa (2012)

$$[e] = \begin{bmatrix} e_1 \\ e_2 \end{bmatrix} = \begin{bmatrix} e_{XX} \\ 2e_{XY} \end{bmatrix} = \begin{bmatrix} (1+u'_x)\cos\theta + u'_y \sin\theta - Y\theta' - 1 \\ -(1+u'_x)\sin\theta + u'_y \cos\theta \end{bmatrix} = \begin{bmatrix} e - Y\kappa \\ \gamma \end{bmatrix} \quad (8)$$

$$e = (1 + u'_X) \cos \theta + u'_Y \sin \theta - 1; \quad \gamma = -(1 + u'_X) \sin \theta + u'_Y \cos \theta; \quad \kappa = \theta' \tag{9}$$

where e is the axial strain, γ is the shear strain and κ is curvature of the beam, $u'_X = du_X/dX$, $u'_Y = du_Y/dX$, $\theta' = d\theta/dX$. The second Piola-Kirchhoff stresses with a temperature rise can be expressed by inclusion of the temperature term as follows

$$s = \begin{bmatrix} s_{XX} \\ s_{XY} \end{bmatrix} = \begin{bmatrix} s_1 \\ s_2 \end{bmatrix} = \begin{bmatrix} s_1^0 + E(Y, T)(e_1 - \alpha_X(Y, T)\Delta T(Y)) \\ s_2^0 + G(Y, T)e_2 \end{bmatrix} \tag{10}$$

$$= \begin{bmatrix} s_1^0 \\ s_2^0 \end{bmatrix} = \begin{bmatrix} E(Y, T) & 0 \\ 0 & G(Y, T) \end{bmatrix} \begin{bmatrix} e_1 - \alpha_X(Y, T)\Delta T(Y) \\ e_2 \end{bmatrix}$$

where s_1^0, s_2^0 are initial stresses, E is Young's modulus and G is the shear modulus, α_X is coefficient of thermal expansion in the X direction and $T = T_0 + \Delta T$, where T_0 is installation temperature and ΔT is the uniform temperature rise.

The temperature $\Delta T = \Delta T(Y)$ is governed by heat transfer equation of

$$-\frac{d}{dY} \left[K(Y) \frac{dT(Y)}{dY} \right] = 0 \tag{11}$$

By integrating Eq. (11) using boundary conditions $T(h/2) = T_T$ and $T(-h/2) = T_B$, the following expression can be obtained

$$\Delta T(Y) = T_B + (T_T - T_B) \int_{-h/2}^Y \frac{1}{K(Y)} dY \bigg/ \int_{-h/2}^{h/2} \frac{1}{K(Y)} dY \tag{12}$$

Using constitutive Eq. (10), axial force N , shear force V and bending moment M can be obtained as

$$N = \int_A s_1 dA = \int_A [s_1^0 + E(Y, T)(e - Y\kappa - \alpha_X(Y, T)\Delta T(Y))] dA \tag{13}$$

$$N = N^0 + A_{xxI}e - B_{xxI}\kappa - N_T \tag{14}$$

$$V = \int_A s_2 dA = \int_A [s_2^0 + G(Y, T)e_2] dA = V^0 + A_{xzt} \gamma \tag{15}$$

$$M = \int_A -Ys_1 dA = \int_A -Y[s_1^0 + E(Y, T)(e - Y\kappa - \alpha_X(Y, T)\Delta T(Y))] dA \tag{16}$$

$$M = M^0 - B_{xxI}e - D_{xxI}\kappa - M_T \tag{17}$$

$$N^0 = \int_{A_0} s_1^0 dA \tag{18a}$$

$$V^0 = \int_{A_0} s_2^0 dA \tag{18b}$$

$$M^0 = \int_{A_0} -Ys_1^0 dA \quad (18c)$$

$$A_{xxt} = \int_A E(Y, T) dA \quad (19a)$$

$$B_{xxt} = \int_A E(Y, T) Y dA \quad (19b)$$

$$D_{xxt} = \int_A E(Y, T) Y^2 dA \quad (19c)$$

$$A_{xzt} = \int_A G(Y, T) dA \quad (20)$$

$$(N_T, M_T) = \int_A E(Y, T) \alpha(Y, T) \Delta T(Y) (1, Y) dA \quad (21)$$

where A_{xxt} , B_{xxt} , D_{xxt} and A_{xzt} , are the extensional, coupling, bending and transverse shear rigidities, respectively. N_T and M_T are the thermal axial force and the bending moment, respectively.

For the solution of the total Lagrangian formulations of TL Timoshenko beam problem, small-step incremental approaches from known solutions are used. As it is known, it is possible to obtain solutions in a single increment of the external force only in the case of mild nonlinearity (and no path dependence). To obtain realistic answers, physical insight into the nature of the problem and, usually, small-step incremental approaches from known solutions are essential. Such increments are always required if the constitutive law relating stress and strain changes is path dependent. Also, such incremental procedures are useful to reduce excessive numbers of iterations and in following the physically correct path. In the iterations, the temperature loading is divided by a suitable number according to the value of temperature. In high temperature values, the temperature loading is divided by large numbers. After completing an iteration process, the load is increased by adding load increment to the accumulated load.

In this study, small-step incremental approaches from known solutions with Newton-Raphson iteration method are used in which the solution for $n + 1$ th load increment and i th iteration is obtained in the following form

$$du_n^i = (K_T^i)^{-1} R_{n+1}^i \quad (22)$$

where $(K_T^i)_S$ is the system stiffness matrix corresponding to a tangent direction at the i th iteration, du_n^i is the solution increment vector at the i th iteration and $n + 1$ th load increment, $(R_{n+1}^i)_S$ is the system residual vector at the i th iteration and $n + 1$ th load increment. This iteration procedure is continued until the difference between two successive solution vectors is less than a selected tolerance criterion in Euclidean norm given by

$$\sqrt{\frac{[(du_n^{i+1} - du_n^i)^T (du_n^{i+1} - du_n^i)]^2}{[(du_n^{i+1})^T (du_n^{i+1})]^2}} \leq \zeta_{tol} \quad (23)$$

A series of successive approximations gives

$$u_{n+1}^{i+1} = u_{n+1}^i + du_{n+1}^i = u_n + \Delta u_n^i \tag{24}$$

where

$$\Delta u_n^i = \sum_{k=1}^i du_n^k \tag{25}$$

The residual vector R_{n+1}^i for a finite element is as follows

$$R_{n+1}^i = f - p \tag{26}$$

where f is the vector of external forces and p is the vector of internal forces given in Appendix.

The element tangent stiffness matrix for the total Lagrangian Timoshenko plane beam element is as follows which is given by Kocatürk and Akbaş (2011) and Felippa (2012)

$$K_T = K_M + K_G \tag{27}$$

where K_G is the geometric stiffness matrix, and K_M is the material stiffness matrix given as follows by Kocatürk and Akbaş (2011) and Felippa (2012)

$$K_M = \int_{L_0} B_m^T S B_m dX \tag{28}$$

The explicit forms of the expressions in Eq. (27) is given in Appendix. After integration of Eq. (28), K_M can be expressed as follows

$$K_M = K_M^a + K_M^b + K_M^s \tag{29}$$

where K_M^a is the axial stiffness matrix, K_M^b is the bending stiffness matrix, K_M^s is the shearing stiffness matrix and explicit forms of these expressions remain the same as given by Kocatürk and Akbaş (2011) except for modulus of elasticity E depends on temperature T in the present study. As defined before, A_{xxt} , B_{xxt} , D_{xxt} and A_{xzt} are the extensional, coupling, bending and transverse shear rigidities, respectively. A_{xxt} appears in the matrix K_M^a , D_{xxt} appear in the matrix K_M^b , A_{xzt} appear in the matrix K_M^s .

The geometric stiffness matrix K_G , B_m and the internal nodal force vector p remains the same as given by Kocatürk and Akbaş (2011) and Felippa (2012) and given in Appendix.

After obtaining the displacements of nodes, the second Piola-Kirchhoff stress tensor components S_{xx} , S_{xy} , S_{yy} can be obtained by using Eq. (10). The relation between the Cauchy stress tensor components σ_{xx} , σ_{xy} , σ_{yy} and the second Piola-Kirchhoff stress tensor components S_{xx} , S_{xy} , S_{yy} is given in Kocatürk and Akbaş (2011).

The beams considered in numerical examples are elastic, with undeformed length L , rectangular cross-section of width b and thickness h (see Fig. 1).

3. Numerical results

In the numerical examples, the post-buckling deflections as well as the maximum. Cauchy normal stresses, critical buckling temperatures are calculated and presented in figures for temperature dependent and independent physical properties for various thermal loads. To this end, by use of usual assembly process, the system tangent stiffness matrix and the system residual vector are obtained by using the element stiffness matrixes and element residual vectors for the total Lagrangian Timoshenko plane beam element. After that, the solution process outlined in the previous section is used for obtaining the related solutions for the total Lagrangian finite element model of Timoshenko plane beam element. the numerical integrations, five-point Gauss integration rule is used.

In Table 1, the central deflections $V(L/2)$ of the beam for uniform temperature rise $\Delta T = 35 K$, $n = 0$ are calculated for various numbers of finite elements x_n for $L/h = 80$, $b = 1$ m, $h = 1$ m with temperature-dependent physical properties. Where, temperature rise $\Delta T = 35 K$ corresponds to yield temperature for $L/h = 80$ in the post-buckling case which is plotted in Fig. 11a.

It is seen from Table 1 that, when the number of finite elements is $x_n = 120$, the considered displacements converge. Therefore, in the numerical calculations, the number of finite elements is taken as $x_n = 120$.

The beams considered in numerical examples are made of Austenitic Stainless Steel (316) and pure Molybdenum. The bottom surface of the functionally graded beam is pure Molybdenum and the top surface of the functionally graded beam is Austenitic Stainless Steel (316). In this study, the material of the beam is considered in the elastic range, so as not to exceed the yield stress (σ_y) that is a function of temperature. Hence, if the stress of the beam equals to yield stress, then the analysis is interrupted. So, plastic buckling and plastic post-buckling cases are not considered in this study. In numerical examples, the initial temperature (installation temperature) of the beam is assumed to be $T_0 = 300 K$. The height of the beam is $h = 1$ m and the width of the beam is $b = 1$ m.

Table 1 Convergence analysis for the central deflections $V(L/2)$ of the beam for various numbers of finite elements n for $\Delta T = 35 K$, $L/h = 80$ and $n = 0$

<i>The central deflections $V(L/2)$ of the beam</i>	
x_n	$V(L/2)$ (m)
20	0.2349
30	0.2596
40	0.2676
50	0.2712
60	0.2732
70	0.2744
80	0.2750
90	0.2754
100	0.2756
110	0.2757
120	0.2757

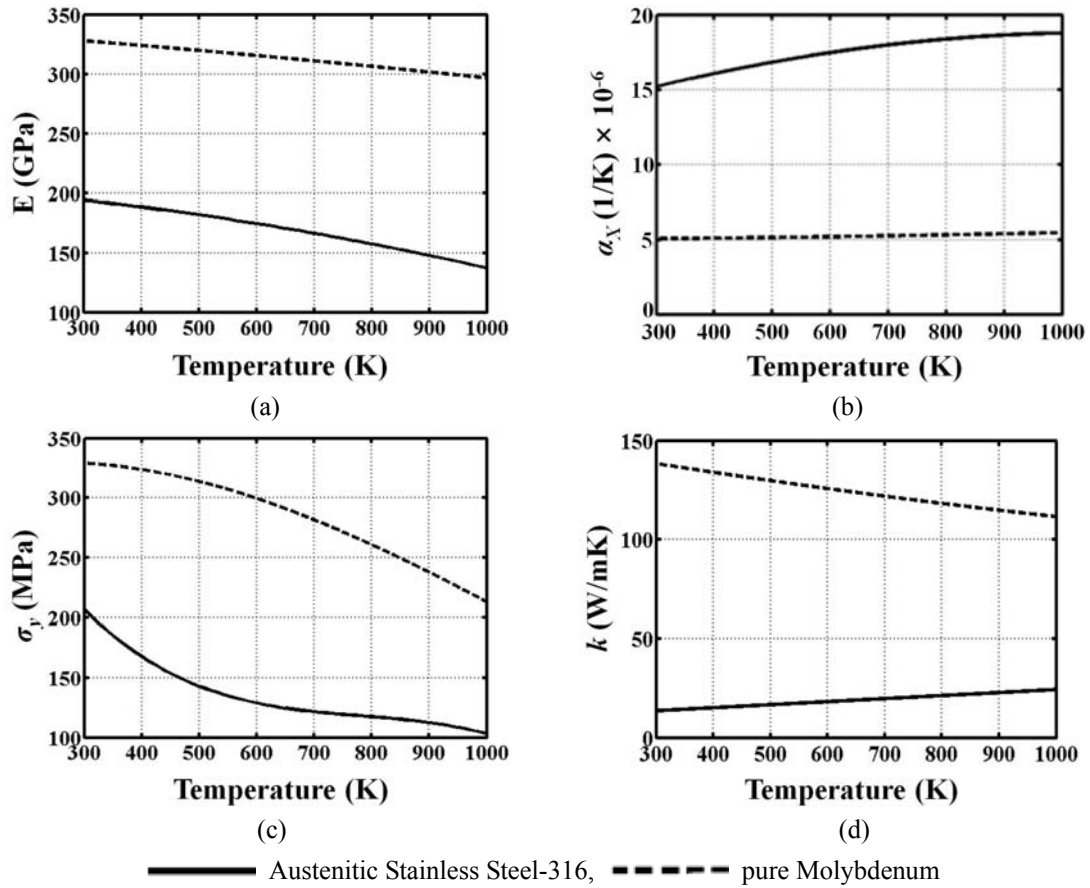


Fig. 4 The material properties versus temperature rising: (a) Young's Modulus; (b) coefficient of thermal expansion; (c) yield stress; (d) coefficient of thermal conductivity

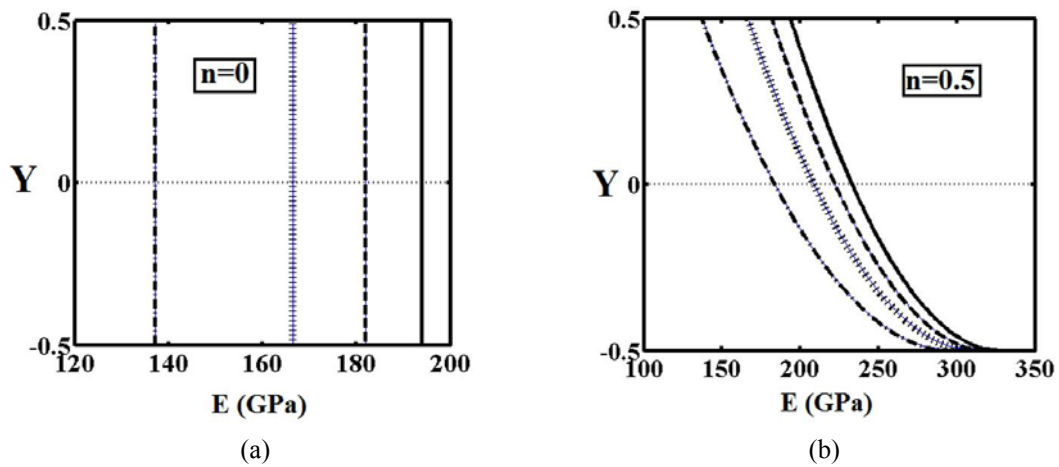


Fig. 5 Variations of Young's Modulus with some given values of the uniform temperature rising: (a) $n = 0$ (Full Austenitic stainless steel (316)); (b) $n = 0.5$; (c) $n = 3$; (d) $n = \infty$ (Full pure Molybdenum)

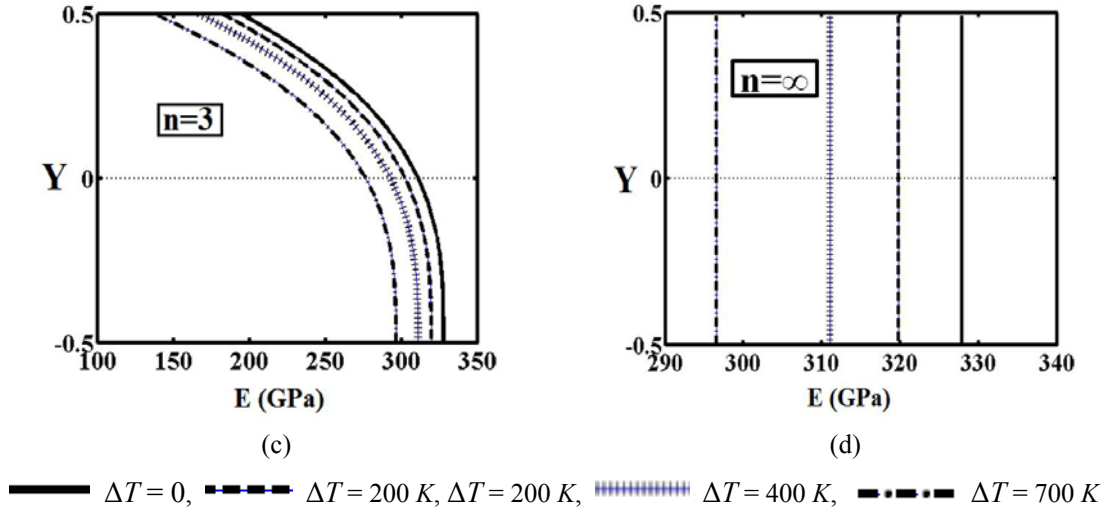


Fig. 5 Continued

stresses (true stresses) can be obtained after obtaining the second Piola-Kirchhoff stresses by using the relations between the Cauchy and the second Piola-Kirchhoff stresses tensor components given by Kocatürk and Akbaş (2011) and Felippa (2012).

Young's Modulus, the coefficient of thermal expansion, yield stress and coefficient of thermal conductivity versus temperature rising are illustrated in Fig. 4 by using Eqs. (2) and (3) for Austenitic Stainless Steel (316) and pure Molybdenum.

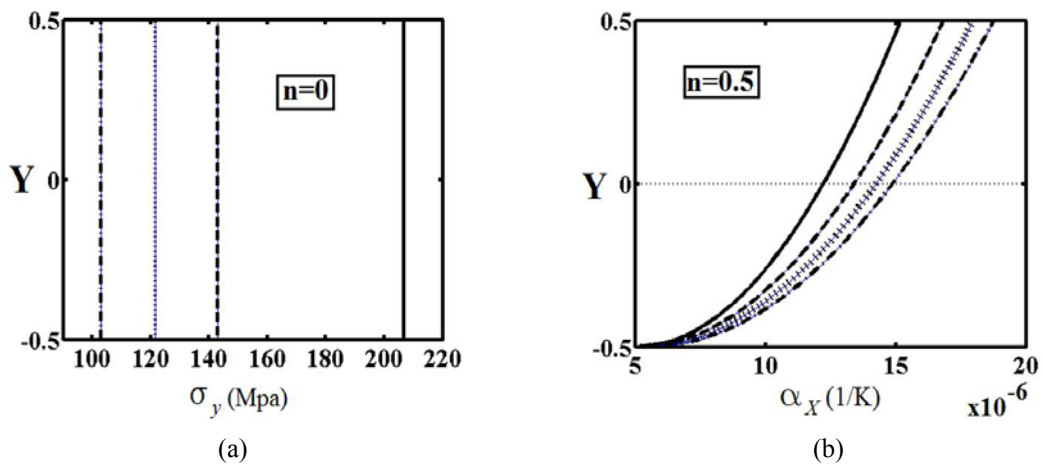


Fig. 6 Variations of the coefficient of thermal expansion with some given values of the uniform temperature rising: (a) $n = 0$ (Full Austenitic stainless steel (316)); (b) $n = 0.5$; (c) $n = 3$; (d) $n = \infty$ (Full pure Molybdenum) and the yield stresses

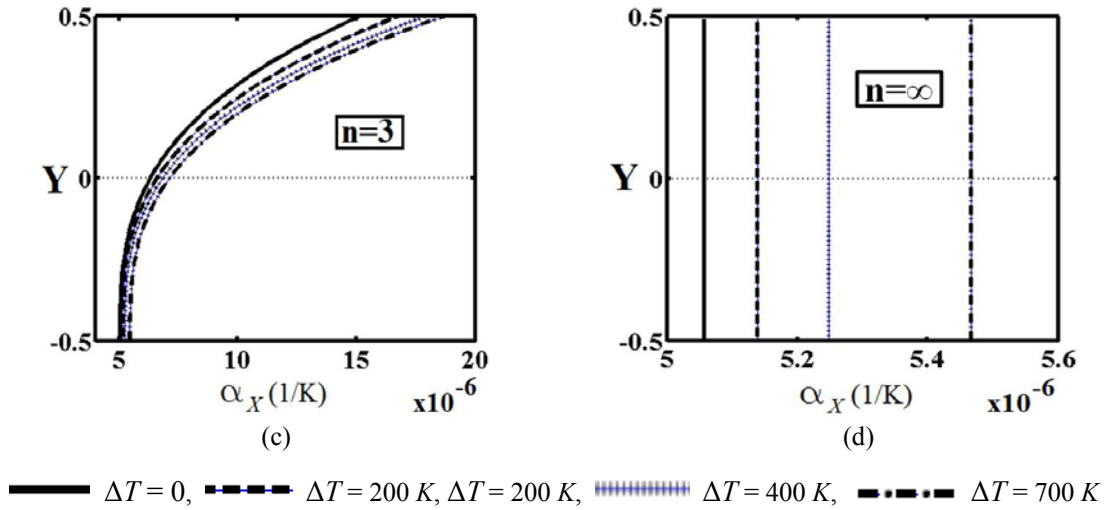


Fig. 6 Continued

It is seen from Fig. 4(a) that with increase in temperature, Young’s modulus decreases. Because, with the temperature increase, the intermolecular distances of the material increase and intermolecular forces decrease. As a result, the strength of the material decreases. It is seen from Fig. 4(b) that, with temperature increase, the coefficient of thermal expansion increases. It is seen from Fig. 4(c) that, increase in temperature causes decrease in the yield stresses. Also, It is seen from Fig. 4 that, with temperature increase, in spite of the coefficient of thermal conductivity of Austenitic stainless steel (316) decreases, but the coefficient of thermal conductivity of pure Molybdenum increases.

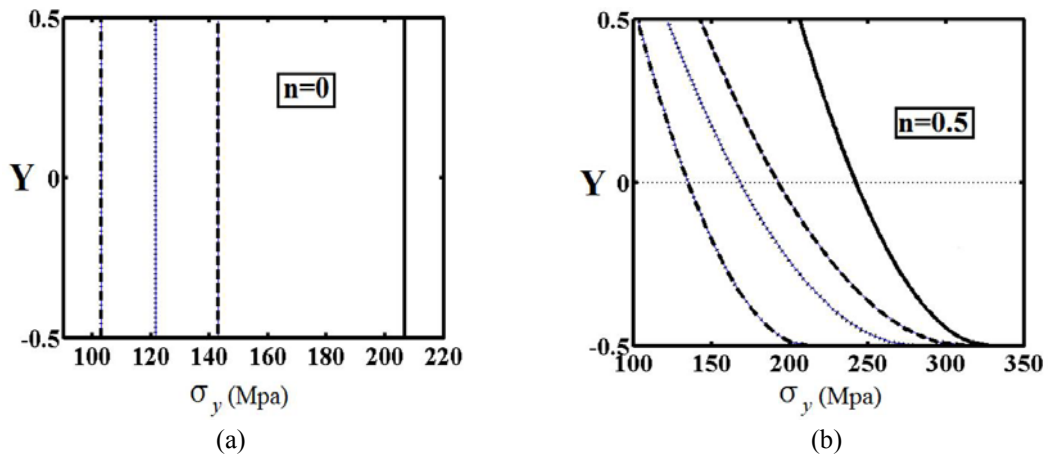
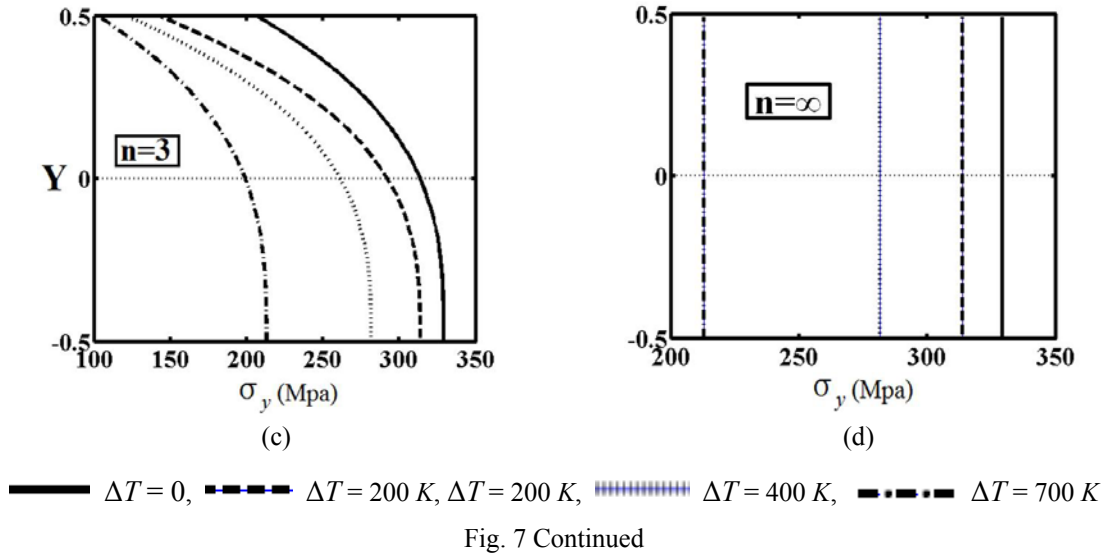


Fig. 7 Variations of the yield stresses with some given values of the uniform temperature rising: (a) $n = 0$ (full austenitic stainless steel (316)); (b) $n = 0.5$; (c) $n = 3$; (d) $n = \infty$ (full pure molybdenum)



In Fig. 5, Figs. 6 and 7, the variations of material properties (Young’s Modulus, the coefficient of thermal expansion and the yield stresses, respectively) distributions along the height of the beam are presented for some given values of the uniform temperature rising ΔT and some given values of the power-law exponent with temperature dependent physical properties.

It is seen from Fig. 5, Figs. 6 and 7 that with increase in temperature, the physical properties of materials varies considerably. Also, It is seen from Figs. 5, 6 and 7 that, the material power law index n play an important role on the properties of the materials.

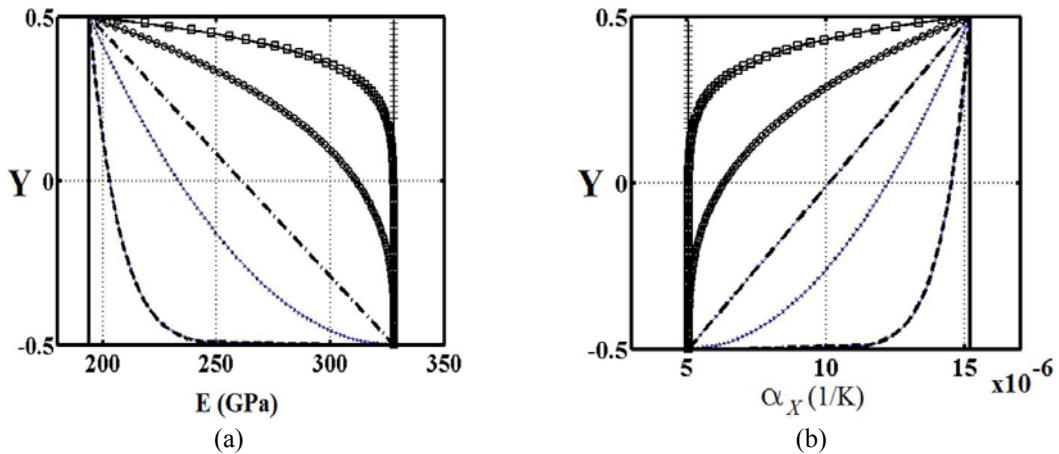


Fig. 8 The material properties distributions along the height of the beam for some given values of the power-law exponent n for for the uniform temperature rising $\Delta T = 700\text{ K}$ for temperature independent physical properties: (a) Young’s Modulus; (b) Coefficient of thermal expansion; (c) the yield stresses; (d) Coefficient of thermal conductivity k

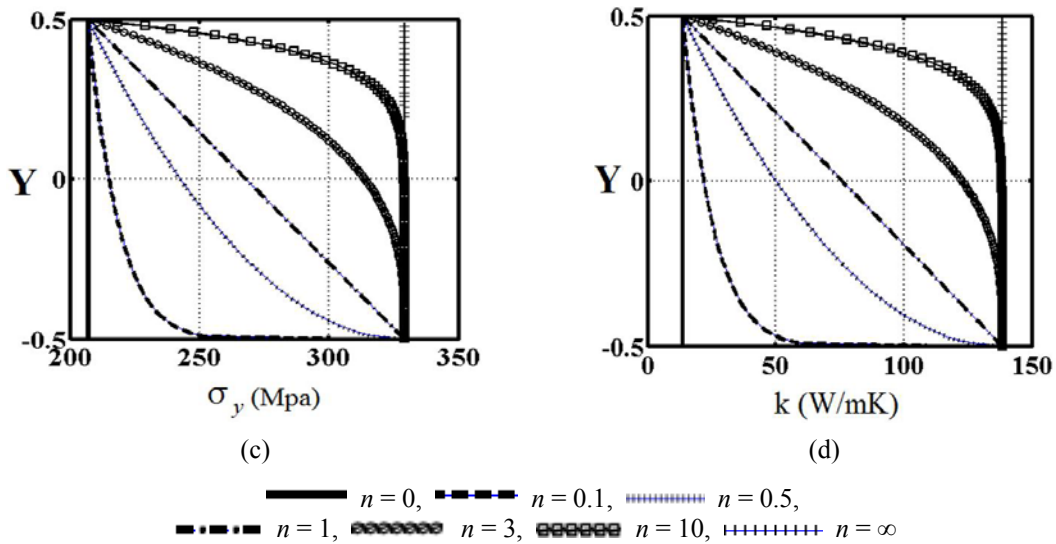


Fig. 8 Continued

In Figs. 8 and 9, the variations of material properties (Young's Modulus, the coefficient of thermal expansion, the yield stresses and the coefficient of thermal conductivity, respectively) distributions along the height of the beam are presented for some given values of the power-law exponent n for the uniform temperature rising $\Delta T = 700 K$ for temperature independent and temperature dependent physical properties respectively.

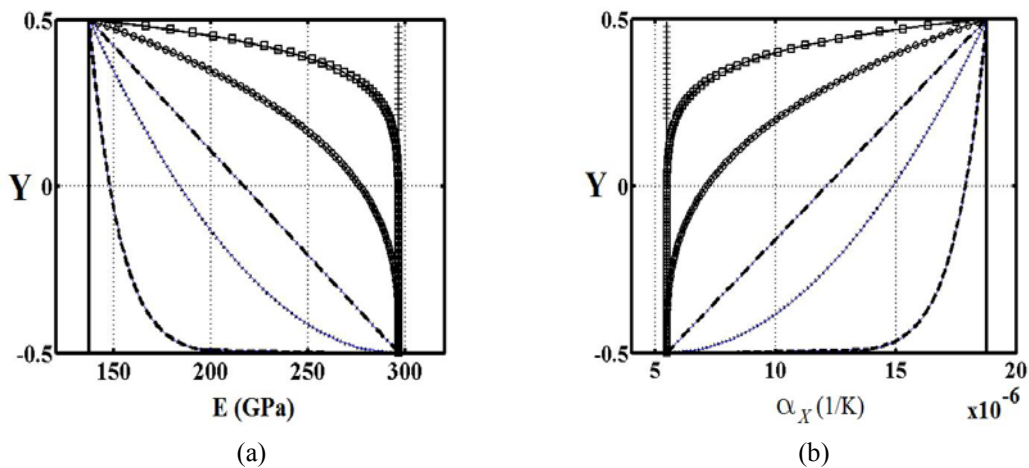


Fig. 9 The material properties distributions along the height of the beam for some given values of the power-law exponent n for for the uniform temperature rising $\Delta T = 700 K$ for temperature dependent physical properties; (a) Young's Modulus; (b) Coefficient of thermal expansion; (c) the yield stress; (d) Coefficient of thermal conductivity k

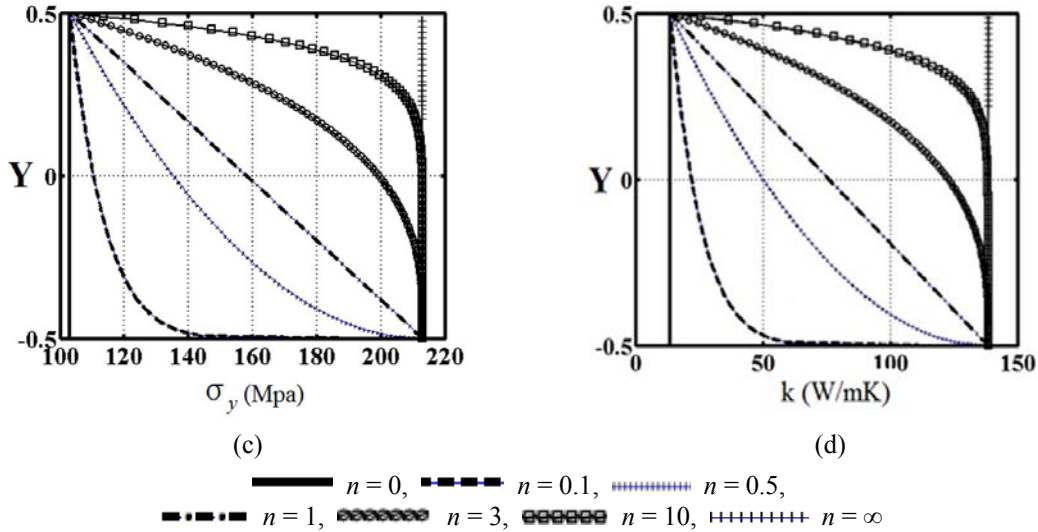


Fig. 9 Continued

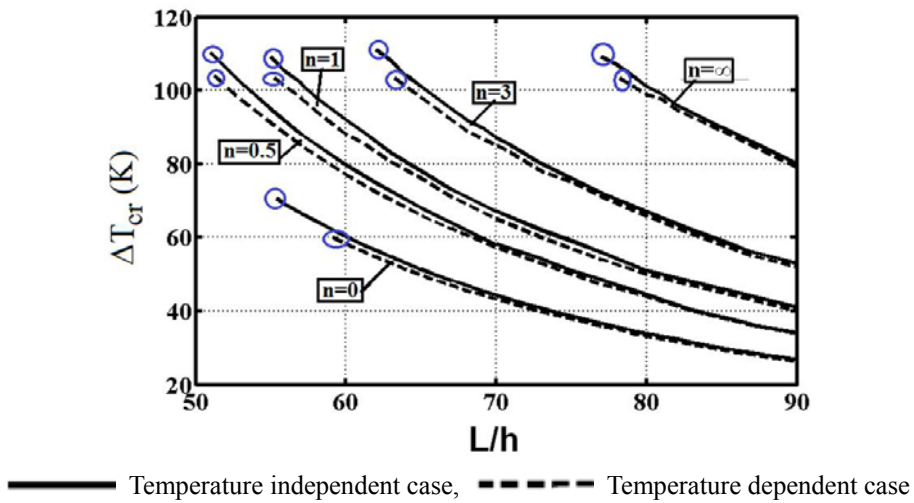


Fig. 10 Critical buckling uniform temperature $\Delta T_{cr}(K)$ versus the ratio L/h and some given values of the power-law exponent n for temperature dependent and independent physical properties for $b = 1$ m and $h = 1$ m

It is seen from Figs. 8 and 9 that, when the material power law index n increases, Young's modulus and the yields stress decreases, the coefficient of thermal expansion decreases. As a result, the strength of the material decreases with increase the power law index n . Because when the material power law index n increase, the material of the beam get close to the pure Molybdenum and it is known from the physical properties of the pure Molybdenum and Austenitic stainless steel (316) that the Young modulus and the yields stress of pure Molybdenum is approximately greater

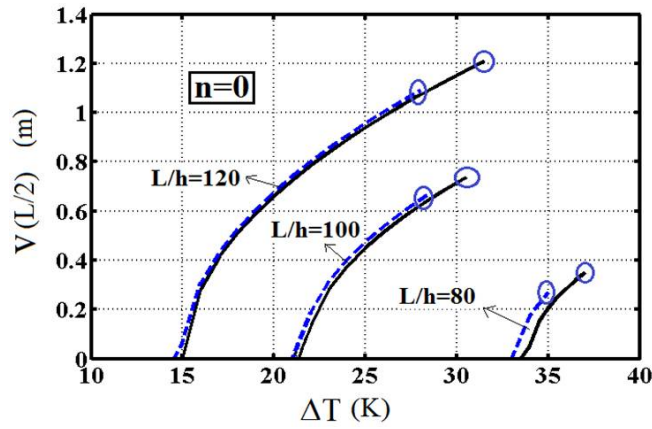
than that of Austenitic stainless steel (316). Also, It is seen from Figs. 8 and 9 that, the selection of power law index n may play an important role in the responses. It can be seen from Figs. 8 and 9 that there are very significant differences between the temperature independent and temperature dependent physical properties.

In Fig. 10, the critical buckling uniform temperature ΔT versus the ratio L/h of the beam and some given values of the power-law exponent n is presented for temperature dependent and independent physical properties for $b = 1$ m and $h = 1$ m.

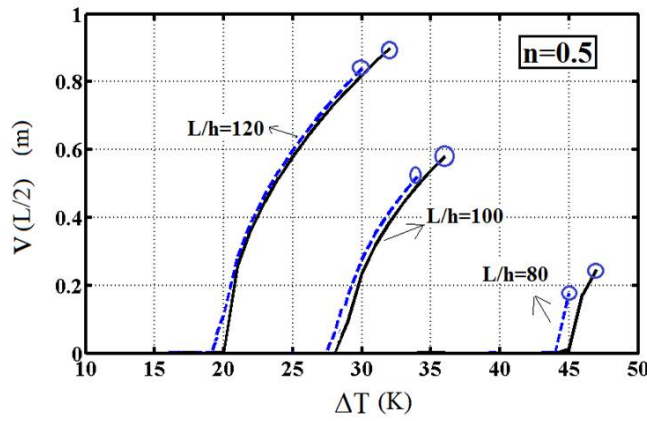
It seen from Fig. 10 that, the beam buckles at lower temperatures for higher L/h ratios for temperature dependent case. when the material power law index n increases, the beam buckles at high temperatures: Because when the material power law index n increase, the material of the beam get close to the pure Molybdenum and it is known from the physical properties of the pure Molybdenum and Austenitic stainless steel (316) that the strength of pure Molybdenum is approximately greater than that of Austenitic stainless steel (316). Hence, the beam buckles at high temperatures with increase the material power law index n . Also it is seen Fig. 10 that, decrease of the ratio L/h of the beam causes increase in the difference between the critical buckling temperatures for the temperature dependent and independent physical properties. In small L/h ratios, the critical temperatures for the temperature-independent physical properties are greater than the critical temperatures of the temperature-dependent physical properties. In Fig. 10, the elastic buckling limits are shown by circles. It is mentioned before that, the material of the beam is considered in the elastic range, so as not to exceed the yield stress. Hence, if the stress of the beam equals to yield stress, then the analysis is interrupted. So, plastic buckling and plastic post-buckling cases are not considered in this study. It is seen Fig. 10 that, the temperature-dependent physical properties must be taken. In Fig. 10, an another interesting point that increase the material power law index n increases, the elastic limits of temperature dependent and independent cases are converge.

In Fig. 11, the specified transversal displacement $V(L/2)$ versus uniform temperature rising ΔT is presented for temperature dependent and independent physical properties for $L/h = 80, 90, 100$ ratios and some given the material power law index n .

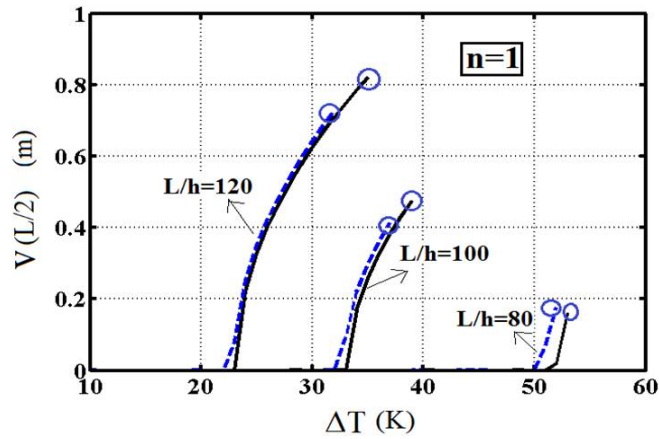
It is seen from Fig. 11 that the difference of the transversal displacements of the midpoint of the beam with the temperature dependent and independent physical properties in post-buckling case increases with decrease in the ratio L/h . It is mentioned before that, if temperature dependent physical properties are not considered in the design of structural elements, there will be an important error. Also, it is seen from Fig. 11 that increase in the material power law index n generally causes increase in the deflections and the beam buckles at high temperatures: Because when the material power law index n increase, the material of the beam get close to the pure Molybdenum and it is known from the physical properties of the pure Molybdenum and Austenitic stainless steel (316) that the strength of pure Molybdenum is approximately greater than that of Austenitic stainless steel (316). In Fig. 8, furcation points can be seen. As it is known, buckling occurs at the furcation points: Actually these points are bifurcation points. As it is known, according to the initial arbitrary deviation from the straight position of the beam, buckling can occur in either positive or negative directions. In this study, deviation from the straight position is always taken as positive for buckling analysis. The symmetrical branches according to ΔT axis would be obtained if the deviations from the straight positions were taken as negative values. The transversal displacements for the temperature-dependent physical properties are greater than those for the temperature-independent physical properties. Also, it is seen from Fig. 11 that the material of the beam yields after certain temperatures that are shown by circles on the figures in the post-



(a)



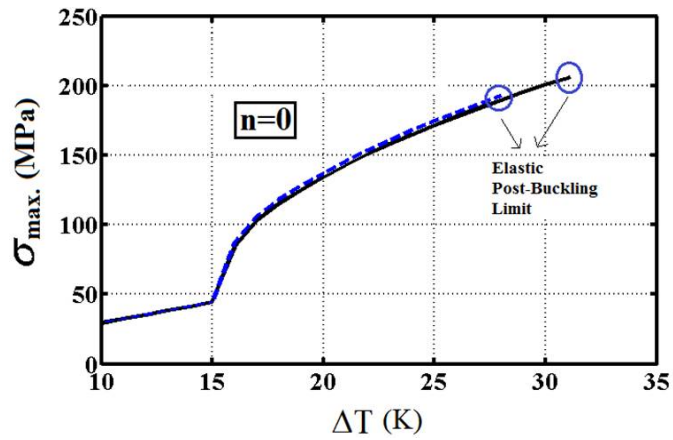
(b)



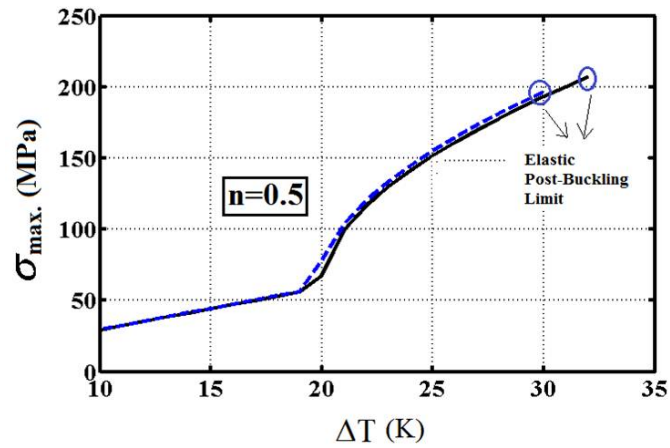
(c)

— Temperature independent case, - - - Temperature dependent case

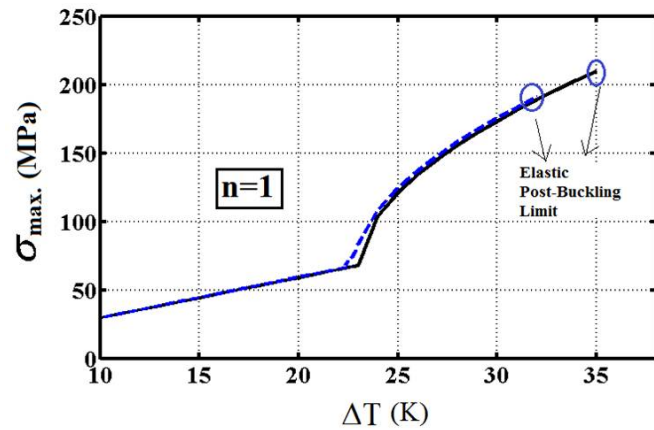
Fig. 11 The specified transversal displacement $V(L/2)$ versus uniform temperature rising ΔT with temperature dependent and independent physical properties for $L/h = 80, 90, 100$ ratios: (a) $n = 0$; (b) $n = 0.5$ and (c) $n = 1$



(a)



(b)



(c)

— Temperature independent case, - - - - - Temperature dependent case

Fig. 12 Maximum Cauchy normal stress versus uniform temperature rising ΔT for temperature dependent and independent physical properties for some given the material power law index n for $L/h = 120$, $b = 1$ m and $h = 1$ m: (a) $n = 0$; (b) $n = 0.5$ and (c) $n = 1$

buckling case: After the corresponding temperature, plasticity must be considered which is out of the scope of this study.

In Fig. 12, maximum Cauchy normal stresses versus uniform temperature rising ΔT is presented for temperature dependent and independent physical properties for some given the material power law index n for $L/h = 120$, $b = 1$ m and $h = 1$ m.

The maximum Cauchy normal stresses for the temperature dependent and independent physical properties in the post-buckling case within elastic limit are given in Fig. 9. Also, it is seen from Fig. 12 that increase in the material power law index, the beam buckles at high temperature. Before the buckling furcation point, the maximum Cauchy normal stresses increase almost linearly, but after furcation point, the stresses increase suddenly. This situation is expected and natural in buckling phenomenon. Also, it is seen from Fig. 9 that the yield stress for the beam with temperature dependent physical properties is lower than the yield stress for the beam with temperature independent physical properties.

4. Conclusions

Thermal post-buckling analysis of functionally graded Timoshenko beams subjected to temperature rising is investigated for temperature dependent and temperature independent physical properties by using the total Lagrangian Timoshenko beam element approximation. Material properties of the beam change in the thickness direction according to a power-law function. The considered highly non-linear problem is solved considering full geometric non-linearity by using incremental displacement-based finite element method in conjunction with Newton-Raphson iteration method. The difference between the analysis results for the temperature dependent and independent physical properties are investigated in detail in post-buckling case. The relationships between deflections, critical buckling temperatures, maximum stresses of the beams and temperature rising are illustrated in detail in post-buckling case.

It is observed from the investigations that there are huge differences of the analysis results for the temperature dependent and temperature independent physical properties for functionally graded beams in the post-buckling case. Especially, increase in temperature causes a huge increase in the difference of the analysis results for the temperature dependent and temperature independent physical properties. The material power law index n and temperature dependent material properties play an important role on the behavior of thermal post-buckling case. Therefore, considering the temperature dependence of the physical properties of beam material and choice of the material power law index n are very important for safe design of functionally graded structures. After certain temperatures, the material of the beam begins yields partially and for increasing temperatures the yield region extends and after certain temperature the beam yields fully and fails in the case of the temperature-dependent physical properties. The yield stresses of material for temperature dependent physical properties are lower than the yield stresses of temperature independent physical properties. Hence, for safe design of structural elements, the temperature-dependent physical properties must be considered. Also, it is seen from the results that functionally graded material has a great performance for high. It is observed from open literature that the effect of temperature dependent physical properties on the analysis results are not considered broadly for functionally graded beams. Taking into consideration of the temperature dependent physical properties is very important for failure analysis and safe design of functionally graded structures.

References

- Akbaş, Ş.D. (2012), "Post-buckling behaviour of functionally graded beams under the influence of temperature", Ph.D. Thesis, Institute of Science at Yıldız Technical University, Istanbul.
- Akbaş, Ş.D. and Kocatürk, T. (2011) "Eksenel Doğrultuda Fonksiyonel derecelendirilmiş Timoshenko kirişinin sıcaklık etkisi altındaki burkulma sonrası davranışının incelenmesi (Post-buckling behavior of axially functionally graded Timoshenko beam under the influence of temperature)", *XVII. Turkish National Mechanics Congress*, Elazığ, Turkey.
- Akbaş, Ş.D. and Kocatürk, T. (2011), "Post-buckling analysis of a simply supported beam under uniform thermal loading", *Scientific Research and Essays*, **6**(4), 1135-1142.
- Akbaş, Ş.D. and Kocatürk, T. (2012), "Post-buckling analysis of Timoshenko Beams with temperature-dependent physical properties under uniform thermal loading", *Struct. Eng. Mech., Int. J.*, **44**(1), 109-125.
- Akbaş, Ş.D., Kocatürk, T. and Şimşek, M. (2012), "Thermal post-buckling analysis of 2-D beams made of functionally graded material", *International Conference on Mechanics of Nano, Micro and Macro Composite Structures*, Politecnico di Torino, Italy, June.
- Anand Rao, K.S., Gupta, R.K., Ramchandran, P. and Rao, V. (2010), "Thermal post-buckling analysis of uniform slender functionally graded material beams", *Struct. Eng. Mech., Int. J.*, **36**(5), 545-560.
- ASME Code Cases: Nuclear Components (1992), Case N-47-30, Section III, Division 1., ASME Boiler and Pressure Vessel Code.
- Bhangale, R.K. and Ganesan, N. (2006), "Thermoelastic buckling and vibration behavior of a functionally graded sandwich beam with constrained viscoelastic core", *J. Sound Vib.*, **295**(1-2), 294-316.
- Detail of the ITER Outline Design Report (1994), The ITER Machine, Vol. 2, San Diego.
- Farid, M., Zahedinejad, P. and Malekzadeh, P. (2010), "Three-dimensional temperature dependent free vibration analysis of functionally graded material curved panels resting on two-parameter elastic foundation using a hybrid semi-analytic, differential quadrature method", *Mater. Des.*, **31**(1), 2-13.
- Felippa, C.A. (2013), "Notes on nonlinear finite element methods", Retrieved September. <http://www.colorado.edu/engineering/cas/courses.d/NFEM.d/NFEM.Ch10.d/NFEM.Ch10.pdf>
- Hashizume, H. and Miya, K. (1987), "Thermomechanical behaviour of the first wall subjected to plasma disruption", *Fusion Eng. Des.*, **5**(2), 141-154.
- Incropera, F. and DeWitt, D. (1985), *Fundamentals of Heat and Mass Transfer*, (2nd Edition), John Wiley.
- ITER Documentation Series, No. 29 (1991), *Blanket, Shield Design and Material Data Base*, IAEA, Vienna.
- Kapuria, S., Bhattacharyya, M. and Kumar, A.N. (2008), "Theoretical modeling and experimental validation of thermal response of metal-ceramic functionally graded beams", *J. Therm. Stresses*, **31**(8), 759-787.
- Khdeir, A.A. (2001), "Thermal buckling of cross-ply laminated composite beams", *Acta Mech.*, **149**(1-4), 201-213.
- Kiani, Y. and Eslami, M.R. (2010), "Thermal buckling analysis of functionally graded material beams", *Int. J. Mech. Mater. Des.*, **6**(3), 229-238.
- Kocatürk, T. and Akbaş, Ş.D. (2011), "Post-buckling analysis of Timoshenko beams with various boundary conditions under non-uniform thermal loading", *Struct. Eng. Mech., Int. J.*, **40**(3), 347-371.
- Kocatürk, T. and Akbaş, Ş.D. (2012), "Post-buckling analysis of Timoshenko beams made of functionally graded material under thermal loading", *Struct. Eng. Mech., Int. J.*, **41**(6), 775-789.
- Li, S.-R., Zhang, J.-H. and Zhao, Y.-G. (2006), "Thermal Post-Buckling of Functionally Graded Material Timoshenko Beams", *Appl. Math. Mech. (English Edition)*, **27**(6), 803-810.
- Lim, C.W., Yang, Q. and Lu, C.F. (2009), "Two-dimensional elasticity solutions for temperature dependent in-plane vibration of FGM circular arches", *Compos. Struct.*, **90**(3), 323-329.
- Lu, C., Chen, W. and Zhong, Z. (2006), "Two-dimensional thermoelasticity solution for functionally graded thick beams", *Sci. China Series G: Phys., Mech. Astron.*, **49**(4), 451-460.
- Mohammadia, M. and Drydena, J.R., (2008), "Thermal stress in a nonhomogeneous curved beam", *J. Therm. Stresses*, **31**(7), 587-598.
- Na, K.-S. and Kim, J.-H. (2006), "Thermal postbuckling investigations of functionally graded plates using

- 3-D finite element method”, *Finite Elem. Anal. Des.*, **42**(8-9), 749-756.
- Nirmula, K., Upadhyay, P.C., Prucz, J. and Lyons, D. (2006), “Thermo-elastic stresses in composite beams with functionally graded layer”, *J. Reinf. Plast. Comp.*, **25**(12), 1241-1254.
- Rahimi, G.H. and Davoodinik, A.R. (2008), “Thermal Behavior Analysis of the functionally graded Timoshenko’s beam”, *Int. J. Eng. Sci.*, **19**(5-1), 105-113.
- Rastgo, A., Shafie, H. and Allahverdizadeh, A. (2005), “Instability of curved beams made of functionally graded material under thermal loading”, *Int. J. Mech. Mater. Des.*, **2**(1-2), 117-128.
- Sankar, B.V. and Tzeng, J.T. (2002), “Thermal stresses in functionally graded beams”, *AIAA J.*, **40**(6), 1228-1232.
- Shinno, H., Kitajima, M. and Okada, M. (1988), “Thermal stress analysis of high heat flux materials”, *J. Nucl. Mater.*, **155-157**(1), 290-294.
- Song, X. and Li, S. (2008), “Nonlinear stability of fixed-fixed FGM arches subjected to mechanical and thermal loads”, *Adv. Mater. Res.*, **33-37**, 699-706.
- Tietz, T.E. and Wilson, J.W. (1965), *Behaviour and Properties of Refractory Metals*, Arnold Publishing Co., London.
- Wakashima, K., Hirano, T. and Niino, M. (1990), Space applications of advanced structural materials, *ESA*, SP: 303-397.
- Zienkiewicz, O.C. and Taylor, R.L. (2000), *The Finite Element Method*, (5th Edition), **2**, *Solid Mechanics*, Oxford, Butterworth-Heinemann.

Appendix

The components of the material stiffness matrix: the axial stiffness matrix K_M^a , bending stiffness matrix K_M^b and shearing stiffness matrix K_M^s are as follows

$$K_M^a = \frac{E(T)A_0}{L_0} \begin{bmatrix} c_m^2 & c_m s_m & -c_m \gamma_m L_0 / 2 & -c_m^2 & -c_m s_m & c_m \gamma_m L_0 / 2 \\ c_m s_m & s_m^2 & -\gamma_m L_0 s_m / 2 & -c_m s_m & -s_m^2 & -\gamma_m L_0 s_m / 2 \\ -c_m \gamma_m L_0 / 2 & -\gamma_m L_0 s_m / 2 & \gamma_m^2 L_0^2 / 4 & c_m \gamma_m L_0 / 2 & \gamma_m L_0 s_m / 2 & \gamma_m^2 L_0^2 / 4 \\ -c_m^2 & -c_m s_m & c_m \gamma_m L_0 / 2 & c_m^2 & c_m s_m & c_m \gamma_m L_0 / 2 \\ -c_m s_m & -s_m^2 & \gamma_m L_0 s_m / 2 & c_m s_m & s_m^2 & \gamma_m L_0 s_m / 2 \\ -c_m \gamma_m L_0 / 2 & -\gamma_m L_0 s_m / 2 & \gamma_m^2 L_0^2 / 4 & c_m \gamma_m L_0 / 2 & \gamma_m L_0 s_m / 2 & \gamma_m^2 L_0^2 / 4 \end{bmatrix} \quad (A1)$$

$$K_M^b = \frac{E(T)I_0}{L_0} \begin{bmatrix} 0 & 0 & 0 & 0 & 0 & 0 \\ 0 & 0 & 0 & 0 & 0 & 0 \\ 0 & 0 & 1 & 0 & 0 & -1 \\ 0 & 0 & 0 & 0 & 0 & 0 \\ 0 & 0 & 0 & 0 & 0 & 0 \\ 0 & 0 & -1 & 0 & 0 & 1 \end{bmatrix} \quad (A2)$$

$$K_M^s = \frac{G(T)A_0}{L_0} \begin{bmatrix} s_m^2 & -c_m s_m & -\alpha_1 L_0 s_m / 2 & -s_m^2 & c_m s_m & \alpha_1 L_0 s_m / 2 \\ -c_m s_m & c_m^2 & -c_m \alpha_1 L_0 / 2 & c_m s_m & -c_m^2 & -c_m \alpha_1 L_0 / 2 \\ -\alpha_1 L_0 s_m / 2 & c_m \alpha_1 L_0 / 2 & \alpha_1^2 L_0^2 / 4 & \alpha_1 L_0 s_m / 2 & -c_m \alpha_1 L_0 / 2 & \alpha_1^2 L_0^2 / 4 \\ -s_m^2 & c_m s_m & \alpha_1 L_0 s_m / 2 & s_m^2 & -c_m s_m & \alpha_1 L_0 s_m / 2 \\ c_m s_m & -c_m^2 & -c_m \alpha_1 L_0 / 2 & -c_m s_m & c_m^2 & -c_m \alpha_1 L_0 / 2 \\ -\alpha_1 L_0 s_m / 2 & -c_m \alpha_1 L_0 / 2 & \alpha_1^2 L_0^2 / 4 & \alpha_1 L_0 s_m / 2 & -c_m \alpha_1 L_0 / 2 & \alpha_1^2 L_0^2 / 4 \end{bmatrix} \quad (A3)$$

where m stands for beam midpoint, $\zeta = 0$, and $\theta_m = (\theta_1 + \theta_2) / 2$, $\omega_m = \theta_m + \varphi$, $c_m = \cos \omega_m$, $s_m = \sin \omega_m$, $e_m = L \cos (\theta_m - \psi) / L_0$, $\alpha_1 = 1 + e_m$ and $\gamma_m = L \sin (\psi - \theta_m) / L_0$ (See Fig. A1 for symbols). The axis of the considered beam initially is taken as horizontal, therefore $\varphi = 0$. The matrix S is defined as follows

$$S = \begin{bmatrix} E(T)A_0 & 0 & 0 \\ 0 & G(T)A_0 & 0 \\ 0 & 0 & I_0 A_0 \end{bmatrix} \quad (A4)$$

B_m matrix is as follows

$$B_m = B|_{\zeta=0} = \frac{1}{L_0} \begin{bmatrix} -c_m & -s_m & -\frac{1}{2} L_0 \gamma_m & c_m & s_m & -\frac{1}{2} L_0 \gamma_m \\ s_m & -c_m & \frac{1}{2} L_0 (1 + e_m) & s_m & -c_m & \frac{1}{2} L_0 (1 + e_m) \\ 0 & 0 & -1 & 0 & 0 & 1 \end{bmatrix} \quad (A5)$$

where $z^T = [N \ V \ M]$. The external nodal force vector can be expressed as follows

$$f = h_e \int_h \int_{L_0} \begin{bmatrix} 1-\zeta_1 & 0 & 0 \\ 0 & 1-\zeta_1 & 0 \\ 0 & 0 & 1-\zeta_1 \\ 1-\zeta_2 & 0 & 0 \\ 0 & 1-\zeta_2 & 0 \\ 0 & 0 & 1-\zeta_2 \end{bmatrix} \begin{bmatrix} f_X \\ f_Y \\ 0 \end{bmatrix} dX \ dY + b \int_{L_0} \begin{bmatrix} 1-\zeta_1 & 0 & 0 \\ 0 & 1-\zeta_1 & 0 \\ 0 & 0 & 1-\zeta_1 \\ 1-\zeta_2 & 0 & 0 \\ 0 & 1-\zeta_2 & 0 \\ 0 & 0 & 1-\zeta_2 \end{bmatrix} \begin{bmatrix} t_X \\ t_Y \\ m_Z \end{bmatrix} dX \quad (A8)$$

where f_X, f_Y are the body forces, t_X, t_Y, m_Z are the surface loads in the X, Y directions and about the Z axis, h_e is the thickness, h is the height.